AIMS Mathematics, 10(8): 19617–19641.
DOI: 10.3934/math.2025875
Received: 27 May 2025
Revised: 21 July 2025
Accepted: 07 August 2025
Published: 27 August 2025

https://www.aimspress.com/journal/Math

Research article

Bifurcation analysis and optical soliton solutions of the ion sound and Langmuir wave equation using the modified Khater method

Marium Khadim[1], Muhammad Abbas[1,*], Tahir Nazir[1], Alina Alb Lupas[2,*], Muhammad Nadeem Anwar[3] and M. R. Alharthi[4]

[1] Department of Mathematics, University of Sargodha, 40100 Sargodha, Pakistan; leomarium135@gmail.com, tahir.nazir@uos.edu.pk

[2] Department of Mathematics and Computer Science, University of Oradea, 410087 Oradea, Romania

[3] Institute of Education, University of Sargodha, 40100 Sargodha, Pakistan; nadeem.anwar@uos.edu.pk

[4] Department of Mathematics and Statistics, College of Science, Taif University, P. O. Box 11099, Taif 21944, Saudi Arabia; muteb@tu.edu.sa

* **Correspondence:** Email: muhammad.abbas@uos.edu.pk, dalb@uoradea.ro.

Abstract: This research work focused on the modified Khater method to obtain the optical soliton solutions of the ion sound and Langmuir wave equation. The modified Khater approach, which produces a wide variety of solutions for the model under consideration, is regarded as one of the most modern and accurate analytical approach for non-linear evolution equations. The wave transformation was used to translate the governing model into an ordinary differential equation. The optical soliton solutions that were developed exhibit many waveforms, including singular periodic shape, sharp dark soliton, kink, and anti-kink soliton solutions. The outcomes may have a significant impact on applications in mathematical physics and engineering. Using the wave transformation, the dynamical system of the governing equation was obtained, and the theory of the planar dynamical system was used to carry out its bifurcation. The existence of chaotic behaviors in the suggested model was examined by taking into account a perturbed term in the resulting dynamical system. Furthermore, the dynamical system's sensitivity analysis was analyzed.

Keywords: modified Khater method; bifurcation; ion sound and Langmuir wave model; soliton solution
Mathematics Subject Classification: 34G20, 35A20, 35A22, 35R11

1. Introduction

The study of non-linear phenomena has significantly increased recently in a variety of disciplines, including applied sciences, mechanics, engineering, robotics, demography, medicine, and quantum science. Non-linear partial differential equations (PDEs) profoundly impact the examination of non-linear physical sciences. Non-linear occurrences are one of the most amazing topics in modern science. Because of the subtle balance between dispersive and non-linear effects, the soliton is an important area of non-linear physics. Solitons appear in a variety of ways, including pulses, darkness, kinks, envelopes, light breathers, and much more. The concept of soliton solutions is necessary in order to study how telephones, optical fiber, and other communication equipment work. A soliton is an independent entity that maintains its integrity following a contact. Waves propagating in non-linear dispersive media are known as solitary waves [1]. Even when interacting with other solitons, a soliton maintains its shape since it is a distinct, self-sustaining wave. The soliton solutions of non-linear models are therefore of great interest in mathematical physics. The Zoomeron model [2], the Phi-4 model [3], Konopelchenko–Dubrovsky model [4], and others are among the prominent non-linear models that show the presence of soliton solutions. Various techniques have been devised to discover soliton solutions. One of the most recent methods created for determining the precise solution of non-linear evolution equations (NLEE) is the modified Khater method. It was initially put forth by Khater et al. [5] and many authors have since viewed it as a modified auxiliary equation approach. Its main advantages are consistency and simplicity as well as the ability to minimize computing effort, which is indicative to its many uses. This basic approach uses the auxiliary equation as a foundation, but it also uses seven additional techniques that make it useful for getting accurate answers to a range of integer and fractional-order non-linear PDEs. The non-linear PDEs for which this method has been widely used by many writers include the fractional emerging telecom model, Bogoyavlenskii equation system, fractional order Sharma Tasso—Olever equation and non-linear Schrödinger equation (NLSE) [6].

A mathematical method called bifurcation analysis [7, 8] is employed in order to investigate the qualitative change of a system's behavior for a parameter variation. It can be used for the determination of the parameter values of importance that produce significant change of the system behavior as well as to investigate the change of system behavior with the change of one or more parameters. The important combinations of the main parameter values through which this effect occurs due to arbitrarily small parameter perturbation values are called bifurcation points. Bifurcation and chaotic behavior is a fascinating non-linear phenomenon, which has been investigated in some disciplines such as economics, ecology, telecommunications, and engineering. Through investigation of differential equation dynamic behavior, one can identify whether the periodic external perturbations produce notable chaotic behavior in the given equations. By investigating the system's bifurcation, researchers can know more about its dynamics and can forecast how it can act in a variety of different situations. There are some authors who have reviewed the bifurcation analysis of differential equations from the literature. For example, Jhangeer et al. [9] investigated bifurcation analysis and pattern generating analysis for chaos behavior in the case of a travelling wave solution of a non-linear dynamical system. The higher-order NLSE bifurcation analysis was found by Li et al. [10]. Biswas et al. [11] presented bifurcation analysis of the power law non-linearity Boussinesq equation. A study of bifurcation of a system governed by a complex subcritical Ginzburg-Landau equation coupled with global as well as local time delay feedback was discussed by Mezamo et al. [12].

In this paper, the modified Khater technique was utilized to obtain soliton solutions of the ion sound and Langmuir wave equation (ISLW), giving descriptions of the non-linear wave propagation of the wave in the system. The proposed equation has also been studied by various authors to derive exact soliton solutions by using different methodologies. Seadawy et al. [13] investigated the aforementioned model by utilizing the modified Kudryashov method and hyperbolic function method. Baskonus and Bulut [14] used the sine-Gordon expansion method to explore the ISLW model. Recently, Ganie [15] used the improved Kudryashov, the novel Kudryashov, and the $\exp_a$-function techniques to investigate the ISLW model. Each of these methods has its own significance but some limitations also, as compared to the modified Khater method. The modified Kudryashov method only gives singular rational solutions and the hyperbolic function method gives only hyperbolic and periodic solutions while the modified Khater method gives exponential, trigonometric, hyperbolic, rational, and hybrid function solutions.

The sine-Gordon expansion method only produces complex hyperbolic solutions for the ISLW model while the modified Khater method gives a rich variety of soliton solutions. Similarly, on drawing a comparison among improved Kudryashov, the novel Kudryashov, and the exp-function technique and the modified Khater method, it was concluded that apart from offering new and more universal solutions, the modified Khater method also offers a classification system of various types of solutions in terms of the values of certain parameters. More specifically, these kinds of solutions can be useful in the description of certain physical phenomena related to wave propagation in non-linear models with large non-linear and dispersive effects. This study is noteworthy because it applied the modified Khater method to the ISLW equation, a system that had not yet been thoroughly examined using this approach. With this technique, dominant behaviors and soliton formation were obtained and further insight into the underlying dynamics was gained. The optical soliton solutions obtained through this method are novel and have not been discussed in any previous literature for the ISLW equation. These solutions give descriptions of many waveforms such as singular periodic, sharp dark soliton, kink, and anti-kink solitary waveforms.

Bifurcation analysis is an essential method for examining how dynamical systems' qualitative behavior varies with the parameters. Bifurcation, as used in the ISLW model, aids in locating crucial points at which soliton structures may change from stable to chaotic dynamics. The Jacobian matrix is used to classify equilibrium points once the governing equation is transformed into a dynamical system through variable substitution. The ability to map the phase space and comprehend the system's non-linear dynamical transitions through saddle, centere, or cusp point classification provides predictive insight into the behaviour of plasma waves.

Bifurcation analysis was done after solving these equations, and the results indicated that the system is chaotic under some conditions. The chaotic behavior demonstrates the sensitivity of the model to these parameters by showing that even slight variations to the parameters of the system or the initial conditions can result in significantly different outcomes. To examine the influence of variations in initial conditions and properties of the system on final solutions, sensitivity analysis was also performed. The conclusion of the analysis demonstrated the non-linear behavior of the system and the tendency toward complex, unpredictable events, highlighting the importance of close observation of variations in parameters in such model analysis. The overall picture of the complex dynamics of the system was given by the combined results of the soliton solutions, bifurcation analysis, and sensitivity assessment, which demonstrated the system's tendency toward chaotic and non-linear events.

To make reading easy for the readers, the article is broken down into the following subheadings: In Section 2, the governing is given. Section 3 gives the ordinary differential version of the given model. The algorithm of the modified Khater technique is given in Section 4, and the solutions of the problems are given in Section 5 according to the desired approach. Section 6 displays the graphical representation of the modified Khater method. In Section 7, bifurcation analysis of the suggested model is covered. In Section 8 and Section 9, the chaotic behaviors as well as sensitivity analysis of the chosen non-linear structure are discussed, respectively. Lastly, the conclusions from this document are summarized in Section 10.

2. Governing equation

The system of the ISLW model [15] is considered as follows:

$$\begin{cases} iM_t + \frac{1}{2}M_{xx} - NM = 0, \\ N_{tt} - N_{xx} - 2(|M|^2)_{xx} = 0, \end{cases} \tag{2.1}$$

where the electrostatic field excitations are represented by the parameter $M(x,t)$, the normalized density fluctuation by the parameter $N(x,t)$, the temporal coordinate is expressed by t, the space coordinate is implied by x, the Longmuir electric field is represented by $Me^{i\varepsilon_g t}$, while the plasma frequency, which depends on N, is explained by ε_g. The aforementioned system can be used in applied sciences and engineering to study ponderomotive forces, or the average impact of the electromagnetic field on charged particle motion, particularly in high frequency effects.

3. Wave transformation

In this work, the ISLW model is used to discuss the motion of a compressible fluid. The following transformation relation is taken into consideration in order to find precise solutions of the governing system given in Eq (2.1),

$$\begin{cases} M(x,t) = G(\xi)e^{i\gamma}, & \xi = ax + bt, \\ N(x,t) = H(\xi), & \gamma = fx + qt, \end{cases} \tag{3.1}$$

where the free constants a, b, f, and q are to be determined later. Equations (2.1) and (3.1) imply:

$$\begin{cases} \frac{1}{2}a^2G'' + i(b + af)G' - \frac{1}{2}(2q + f^2)G - GH = 0, \\ (b^2 - a^2)H'' - 4a^2(G'^2 + GG'') = 0. \end{cases} \tag{3.2}$$

The first part of Eq (3.2) gives real and imaginary components as:

$$i(b + af)G' = 0, \tag{3.3}$$

$$a^2G'' - (2q + f^2)G - 2GH = 0. \tag{3.4}$$

The Eq (3.3) gives $b = -af$. Two integrations of the second part of Eq (3.2) with regard to ξ yield:

$$H(\xi) = \frac{2}{f^2 - 1}G^2(\xi), \tag{3.5}$$

where $f \neq \pm 1$. Equations (3.4) and (3.5) give:

$$a^2(f^2 - 1)G'' - (f^2 - 1)(2q + f^2)G - 4G^3 = 0. \tag{3.6}$$

4. Description of the modified Khater method

In this paper, the modified Khater technique [16] for creating a new wave pattern in the ISLW model is proposed. The following provides some information on this process in this context:
Step 1: The NLEE for $G(x,t)$ is displayed in the structure below:

$$E(G, G_t, G_x, G_{tt}, G_{xt}, G_{xx}, ...) = 0. \tag{4.1}$$

By using the wave transformation given in Eq (3.1) in Eq (4.1), the following ODE can be constructed.

$$Q(g, bG', aG', b^2G'', a^2G'', baG'', ...) = 0. \tag{4.2}$$

Step 2: The general solution of Eq (4.2) has the following form:

$$G(\xi) = \sum_{n=1}^{m} \phi_n \, \phi^{nY(\xi)}. \tag{4.3}$$

The following auxiliary equation is pacified by $\phi^{nY(\xi)}$, where the constants $\phi_n (n = 0, 1, 2, 3, ..., m)$ are to be found later:

$$Y'(\xi) = \frac{\mu_1 \phi^{-Y(\xi)} + \eta_1 + \rho \phi^{Y(\xi)}}{\ln(\phi)}. \tag{4.4}$$

Step 3: Homogeneous balancing is used to get m.
Step 4: By applying Eqs (4.3) and (4.4) in Eq (4.2) and connecting each term of the same power $\phi^{nY(\xi)}$, where $(n = 0, 1, ...m)$ to zero, a non-linear system of equations can be produced.
Step 5: The exact solution for Eq (4.1) can be obtained by inserting the obtained output and solutions of Eq (4.4) into Eq (4.3). The solution of Eq (4.4) has the following cases:

If $\eta_1^2 - \mu_1 \, \rho < 0$ and $\rho \neq 0$, then

$$\phi^{Y(\xi)} = -\frac{\eta_1}{\rho} + \frac{\sqrt{\rho\mu_1 - \eta_1^2}}{\rho} \tan\left(\frac{\sqrt{\rho\mu_1 - \eta_1^2}}{2}\xi\right),$$

or

$$\phi^{Y(\xi)} = -\frac{\eta_1}{\rho} + \frac{\sqrt{\rho\mu_1 - \eta_1^2}}{\rho} \cot\left(\frac{\sqrt{\rho\mu_1 - \eta_1^2}}{2}\xi\right). \tag{4.5}$$

If $\eta_1^2 - \mu_1\rho > 0$ and $\rho \neq 0$, then

$$\phi^{Y(\xi)} = -\frac{\eta_1}{\rho} - \frac{\sqrt{\eta_1^2 - \rho\mu_1}}{\rho} \tanh\left(\frac{\sqrt{\eta_1^2 - \rho\mu_1}}{2}\xi\right),$$

or

$$\phi^{Y(\xi)} = -\frac{\eta_1}{\rho} - \frac{\sqrt{\eta_1^2 - \rho\mu_1}}{\rho} \coth\left(\frac{\sqrt{\eta_1^2 - \rho\mu_1}}{2}\xi\right). \tag{4.6}$$

If $\eta_1^2 + \mu_1^2 > 0$, and $\rho \neq 0$, and $\rho = \mu_1$, then

$$\phi^{Y(\xi)} = \frac{\eta_1}{\rho} + \frac{\sqrt{\eta_1^2 + \mu_1^2}}{\mu_1} \tanh(\frac{\sqrt{\eta_1^2 + \mu_1^2}}{2}\xi),$$

or

$$\phi^{Y(\xi)} = \frac{\eta_1}{\rho} + \frac{\sqrt{\eta_1^2 + \mu_1^2}}{\mu_1} \coth(\frac{\sqrt{\eta_1^2 + \mu_1^2}}{2}\xi). \tag{4.7}$$

If $\eta_1^2 + \mu_1^2 < 0$, and $\rho \neq 0$, and $\rho = \mu_1$, then

$$\phi^{Y(\xi)} = \frac{\eta_1}{\rho} - \frac{\sqrt{-(\eta_1^2 + \mu_1^2)}}{\mu_1} \tan(\frac{\sqrt{-(\eta_1^2 + \mu_1^2)}}{2}\xi),$$

or

$$\phi^{Y(\xi)} = \frac{\eta_1}{\rho} - \frac{\sqrt{-(\eta_1^2 + \mu_1^2)}}{\mu_1} \coth(\frac{\sqrt{-(\eta_1^2 + \mu_1^2)}}{2}\xi). \tag{4.8}$$

If $\eta_1^2 - \mu_1^2 < 0$ and $\rho = \mu_1$, then

$$\phi^{Y(\xi)} = -\frac{\eta_1}{\rho} + \frac{\sqrt{-(\eta_1^2 - \mu_1^2)}}{\mu_1} \tanh(\frac{\sqrt{-(\eta_1^2 - \mu_1^2)}}{2}\xi),$$

or

$$\phi^{Y(\xi)} = -\frac{\eta_1}{\rho} + \frac{\sqrt{-(\eta_1^2 - \mu_1^2)}}{\mu_1} \coth(\frac{\sqrt{-(\eta_1^2 - \mu_1^2)}}{2}\xi). \tag{4.9}$$

If $\eta_1^2 - \mu_1^2 > 0$ and $\rho = \mu_1$, then

$$\phi^{Y(\xi)} = -\frac{\eta_1}{\rho} + \frac{\sqrt{\eta_1^2 - \mu_1^2}}{\mu_1} \tanh(\frac{\sqrt{\eta_1^2 - \mu_1^2}}{2}\xi),$$

or

$$\phi^{Y(\xi)} = -\frac{\eta_1}{\rho} + \frac{\sqrt{\eta_1^2 - \mu_1^2}}{\mu_1} \coth(\frac{\sqrt{\eta_1^2 - \mu_1^2}}{2}\xi). \tag{4.10}$$

If $\mu_1\rho < 0$, and $\rho \neq 0$, and $\eta_1 = 0$, then

$$\phi^{Y(\xi)} = \sqrt{-\frac{\mu_1}{\rho}} \tanh(\frac{\sqrt{-\mu_1\rho}}{2}\xi),$$

or

$$\phi^{Y(\xi)} = \sqrt{-\frac{\mu_1}{\rho}} \coth(\frac{\sqrt{-\mu_1\rho}}{2}\xi). \tag{4.11}$$

If $\mu_1 = -\rho < 0$ and $\eta_1 = 0$, then

$$\phi^{Y(\xi)} = \frac{-(1 + e^{2\mu_1\xi}) \pm \sqrt{2(e^{4\mu_1\rho} + 1)}}{e^{2\mu_1\xi} - 1},$$

or

$$\phi^{Y(\xi)} = \frac{-(1+e^{2\mu_1\xi}) \pm \sqrt{e^{4\mu_1\rho}+6e^{2\mu_1\rho}+1}}{2e^2\mu_1\xi}. \tag{4.12}$$

If $\mu_1 = \rho = 0$, then

$$\phi^{Y(\xi)} = \frac{-(1+e^{2\eta_1\xi}) \pm \sqrt{(e^{4\eta_1\rho}+1)}}{e^{2\eta_1\xi}-1},$$

or

$$\phi^{Y(\xi)} = \frac{-(1+e^{2\eta_1\xi}) \pm \sqrt{e^{4\eta_1\rho}+6e^{2\eta_1\rho}+1}}{2e^{2\eta_1\xi}}. \tag{4.13}$$

If $\eta_1^2 = \mu_1\rho$, then

$$\phi^{Y(\xi)} = \frac{-\mu_1(\eta_1\xi+2)}{\eta_1^2\xi}. \tag{4.14}$$

If $\eta_1 = \mu_1 = \rho \neq 0$, then

$$\phi^{Y(\xi)} = \frac{-(\mu_1\xi+2)}{\mu_1\xi}. \tag{4.15}$$

If $\eta_1 = f,\ \mu_1 = 2f$, and $\rho = 0$, then

$$\phi^{Y(\xi)} = e^{f\xi} - 1. \tag{4.16}$$

If $\mu_1 = 0$, then

$$\phi^{Y(\xi)} = \frac{\eta e^{\eta_1\rho}}{1+\frac{\rho}{2}e^{\eta_1\xi}}. \tag{4.17}$$

If $2\eta_1 = \mu_1 + \rho$, then

$$\phi^{Y(\xi)} = \frac{1-\mu_1 e^{\frac{1}{2}(\mu_1-\rho)\xi}}{1-\rho e^{\frac{1}{2}(\mu_1-\rho)\xi}},$$

or

$$\phi^{Y(\xi)} = \frac{\mu_1 e^{\frac{1}{2}(\mu_1-\rho)\xi}+1}{-\rho e^{\frac{1}{2}(\mu_1-\rho)\xi}+1}. \tag{4.18}$$

If $-2\eta_1 = \mu_1 + \rho$, then

$$\phi^{Y(\xi)} = \frac{e^{\frac{1}{2}(\mu_1-\rho)\xi}+\mu_1}{e^{\frac{1}{2}(\mu_1-\rho)\xi}+\rho}. \tag{4.19}$$

If $\eta_1 = \rho = 0$, then

$$\phi^{Y(\xi)} = \frac{\mu_1}{2}\xi. \tag{4.20}$$

If $\eta_1 = \mu_1 = 0$, then

$$\phi^{Y(\xi)} = -\frac{2}{\rho\xi}. \tag{4.21}$$

If $\eta_1 = 0$ and $\mu_1 = \rho$, then

$$\phi^{Y(\xi)} = \tan(\frac{\mu_1\xi+C}{2}). \tag{4.22}$$

If $\rho = 0$, then

$$\phi^{Y(\xi)} = e^{\eta_1\xi} - \frac{\mu_1}{2\eta_1}. \tag{4.23}$$

5. Application of the modified Khater method

This subsection uses the modified Khater approach to derive the solitary wave solutions of Eq (3.6). By using Eq (3.6) and keeping G'' and G^3 balanced, the value $m = 1$ is produced. Using $m = 1$ in Eq (4.4) results in

$$G(\xi) = \phi_o + \phi_1 \phi^{Y(\xi)}. \tag{5.1}$$

A system of non-linear algebraic equations is obtained by connecting all terms with identical powers of $\phi^{Y(\xi)}$ to zero and using Eq (4.4) in Eq (4.3):

$$\begin{gathered}
\phi^{0Y} : -a^2\eta_1\mu_1\phi_1 + a^2 f^2\eta_1\mu_1\phi_1 + f^2\phi_o - f^4\phi_o + 2q\phi_o - 2f^2q\phi_o - 4\phi_o^3 = 0,\\
\phi^{Y} : f^2\phi_1 - f^4\phi_1 + 2q\phi_1 - 2f^2q\phi_1 - a^2\eta_1^2\phi_1 + a^2f^2\eta_1^2\phi_1 - 2a^2\rho\mu_1\phi_1 + 2a^2f^2\rho\mu_1\phi_1 - 12\phi_1\phi_o^2 = 0,\\
\phi^{2Y} : -3a^2\rho\eta_1\phi_1 + 3a^2f^2\rho\eta_1\phi_1 - 12\phi_1^2\phi_o = 0,\\
\phi^{3Y} : -2a^2\rho^2\phi_1 + 2a^2f^2\rho^2\phi_1 - 4\phi_1^3 = 0.
\end{gathered}$$

By using the computational software Mathematica 13.2, the system of algebraic equations was solved to produce the unique solution sets.

$$\begin{gathered}
\phi_o = \frac{i\sqrt{-1+f^2}\sqrt{f^2+2q-a^2\eta_1^2-2a^2\rho\mu_1}}{2\sqrt{3}},\\
\phi_1 = \frac{a\sqrt{-1+f^2}\rho}{\sqrt{2}}.
\end{gathered}$$

Using the distinct solutions for Eq (4.4) given by Eqs (4.5)–(4.23) with the above parameters in Eq (4.3) yields solitary wave solutions for Eq (3.6) as:

Case 1: If $\eta_1^2 - \mu_1\,\rho < 0$, and $\rho \neq 0$, then

$$G_1(x,t) = \frac{1}{6}\sqrt{-1+f^2}(i\sqrt{3}\sqrt{f^2+2q-a^2(\eta_1^2+2\rho\mu_1)} + 3\sqrt{2}a(-\eta_1+\sqrt{-\eta_1^2+\rho\mu_1})\tan(\frac{1}{2}\xi\sqrt{-\eta_1^2+\rho\mu_1}), \tag{5.2}$$

or

$$G_2(x,t) = \frac{1}{6}\sqrt{-1+f^2}(i\sqrt{3}\sqrt{f^2+2q-a^2(\eta_1^2+2\rho\mu_1)} + 3\sqrt{2}a(-\eta_1+\sqrt{-\eta_1^2+\rho\mu_1})\cot(\frac{1}{2}\xi\sqrt{-\eta_1^2+\rho\mu_1}).$$

Case 2: If $\eta_1^2 - \mu_1\rho > 0$, and $\rho \neq 0$, then

$$G_3(x,t) = \frac{1}{6}\sqrt{-1+f^2}(i\sqrt{3}\sqrt{f^2+2q-a^2(\eta_1^2+2\rho\mu_1)} - 3\sqrt{2}a(\eta_1+\sqrt{\eta_1^2-\rho\mu_1})\tanh(\frac{1}{2}\xi\sqrt{\eta_1^2-\rho\mu_1}), \tag{5.3}$$

or

$$G_4(x,t) = \frac{1}{6}\sqrt{-1+f^2}(i\sqrt{3}\sqrt{f^2+2q-a^2(\eta_1^2+2\rho\mu_1)} - 3\sqrt{2}a(\eta_1+\sqrt{\eta_1^2-\rho\mu_1})\coth(\frac{1}{2}\xi\sqrt{\eta_1^2-\rho\mu_1}).$$

Case 3: If $\eta_1^2 + \mu_1^2 > 0$, and $\rho \neq 0$, and $\rho = \mu_1$, then

$$G_5(x,t) = \frac{1}{6}\sqrt{-1+f^2}(i\sqrt{3}\sqrt{f^2+2q-a^2(\eta_1^2+2\rho\mu_1)} + 3\sqrt{2}a\rho(\frac{\eta_1}{\rho}+\frac{\sqrt{\eta_1^2+\mu_1^2}}{\mu_1^2})\tanh(\frac{1}{2}\xi\sqrt{\eta_1^2+\mu_1^2}), \tag{5.4}$$

or

$$G_6(x,t) = \frac{1}{6}\sqrt{-1+f^2}(i\sqrt{3}\sqrt{f^2+2q-a^2(\eta_1^2+2\rho\mu_1)} + 3\sqrt{2}a\rho(\frac{\eta_1}{\rho} + \frac{\sqrt{\eta_1^2+\mu_1^2}}{\mu_1^2})\coth(\frac{1}{2}\xi\sqrt{\eta_1^2+\mu_1^2}).$$

Case 4: If $\eta_1^2+\mu_1^2<0$, and $\rho\neq 0$, and $\rho=\mu_1$, then

$$G_7(x,t) = \frac{1}{6}\sqrt{-1+f^2}(i\sqrt{3}\sqrt{f^2+2q-a^2(\eta_1^2+2\rho\mu_1} + (3\sqrt{2}a(\eta_1\mu_1-\rho\sqrt{-\eta_1^2-\mu_1^2})\tan(\frac{1}{2}\xi\sqrt{-\eta_1^2-\mu_1^2}\frac{1}{\mu_1}), \quad (5.5)$$

or

$$G_8(x,t) = \frac{1}{6}\sqrt{-1+f^2}(i\sqrt{3}\sqrt{f^2+2q-a^2(\eta_1^2+2\rho\mu_1} + (3\sqrt{2}a(\eta_1\mu_1-\rho\sqrt{-\eta_1^2-\mu_1^2})\cot(\frac{1}{2}\xi\sqrt{-\eta_1^2-\mu_1^2}\frac{1}{\mu_1}).$$

Case 5: If $\eta_1^2-\mu_1^2<0$ and $\rho=\mu_1$, then

$$G_9(x,t) = \frac{1}{6}\sqrt{-1+f^2}(i\sqrt{3}\sqrt{f^2+2q-a^2(\eta_1^2+2\rho\mu_1)} + 3\sqrt{2}a(-\eta_1\mu_1+\rho\sqrt{-\eta_1^2+\mu_1^2})\tan(\frac{1}{2}\xi\sqrt{-\eta_1^2+\mu_1^2})\frac{1}{\mu_1}),$$

or

$$G_{10}(x,t) = \frac{1}{6}\sqrt{-1+f^2}(i\sqrt{3}\sqrt{f^2+2q-a^2(\eta_1^2+2\rho\mu_1)} + 3\sqrt{2}a(-\eta_1\mu_1+\rho\sqrt{-\eta_1^2+\mu_1^2})\cot(\frac{1}{2}\xi\sqrt{-\eta_1^2+\mu_1^2})\frac{1}{\mu_1}).$$

Case 6: If $\eta_1^2-\mu_1^2>0$ and $\rho=\mu_1$, then

$$G_{11}(x,t) = \frac{1}{6}\sqrt{-1+f^2}(i\sqrt{3}\sqrt{f^2+2q-a^2(\eta_1^2+2\rho\mu_1)} + 3\sqrt{2}a(-\eta_1\mu_1+\rho\sqrt{\eta_1^2-\mu_1^2})\tanh(\frac{1}{2}\xi\sqrt{\eta_1^2-\mu_1^2})\frac{1}{\mu_1}),$$

or

$$G_{12}(x,t) = \frac{1}{6}\sqrt{-1+f^2}(i\sqrt{3}\sqrt{f^2+2q-a^2(\eta_1^2+2\rho\mu_1)} + 3\sqrt{2}a(-\eta_1\mu_1+\rho\sqrt{\eta_1^2-\mu_1^2})\coth(\frac{1}{2}\xi\sqrt{\eta_1^2-\mu_1^2})\frac{1}{\mu_1}).$$

Case 7: If $\mu_1\rho<0$, $\rho\neq 0$ and $\eta_1=0$, then

$$G_{13}(x,t) = \frac{1}{6}\sqrt{-1+f^2}(i\sqrt{3}\sqrt{f^2+2q-a^2(\eta_1^2+2\rho\mu_1)} + 3\sqrt{2}a\rho\sqrt{-\frac{\mu_1}{\rho}}\tanh(\frac{1}{2}\xi\sqrt{-\rho\mu_1}), \quad (5.6)$$

or

$$G_{14}(x,t) = \frac{1}{6}\sqrt{-1+f^2}(i\sqrt{3}\sqrt{f^2+2q-a^2(\eta_1^2+2\rho\mu_1)} + 3\sqrt{2}a\rho\sqrt{-\frac{\mu_1}{\rho}}\tanh(\frac{1}{2}\xi\sqrt{-\rho\mu_1}).$$

Case 8: If $\mu_1 = -\rho < 0$ and $\eta_1 = 0$, then

$$G_{15}(x,t) = \frac{1}{6}\sqrt{-1+f^2}(-3a\sqrt{1+e^{4\rho\mu_1}}\rho + 3a(-\sqrt{2} + \sqrt{1+e^{4\rho\mu_1}})\rho\coth(\xi\mu_1) + i\sqrt{3}\sqrt{f^2+2q-a^2(\eta_1^2+2\rho\mu_1)}),$$

or

$$G_{16}(x,t) = \frac{\sqrt{-1+f^2}(3\sqrt{2}a(-1-e^{2\xi\mu_1}+\sqrt{1+6e^{2\rho\mu_1}+e^{4\rho\mu_1}})\rho + 2i\sqrt{3}e^2\xi\mu_1\sqrt{f^2+2q-a^2(\eta_1^2+2\rho\mu_1}}{12e^2\xi\mu_1}).$$

Case 9: If $\mu_1 = \rho = 0$, then

$$G_{17}(x,t) = \frac{1}{6}\sqrt{-1+f^2}(-3a\sqrt{e^{1+4\rho\eta_1}}\rho + 3a(-\sqrt{2} + \sqrt{e^{1+4\rho\eta_1}})\rho\coth(\xi\eta_1) + i\sqrt{3}\sqrt{f^2+2q-a^2(\eta_1^2+2\rho\mu_1)}),$$

or

$$G_{18}(x,t) = \frac{1}{12}e^{-2\xi\eta_1}\sqrt{-1+f^2}(3\sqrt{2}a(-1-e^{2\xi\eta_1} + \sqrt{1+6e^{2\rho\eta_1}+e^{4\rho\eta_1}})\rho + 2i\sqrt{3}e^{2\xi\eta_1}\sqrt{f^2+2q-a^2(\eta_1^2+2\rho\mu_1)}).$$

Case 10: If $\eta_1^2 = \mu_1\rho$, then

$$G_{19}(x,t) = \frac{1}{6}\sqrt{-1+f^2}(-\frac{3\sqrt{2}a\rho(2+\xi\eta_1)\mu_1}{\xi\eta_1^2} + i\sqrt{3}\sqrt{f^2+2q-a^2(\eta_1^2+2\rho\mu_1)}). \tag{5.7}$$

Case 11: If $\eta_1 = \mu_1 = \rho \neq 0$, then

$$G_{20}(x,t) = \frac{1}{6}\sqrt{-1+f^2}(-3\sqrt{2}a\rho - \frac{6\sqrt{2}a\rho}{\xi\mu_1} + i\sqrt{3}\sqrt{f^2+2q-a^2(\eta_1^2+2\rho\mu_1)}).$$

Case 12: If $\eta_1 = f$, and $\mu_1 = 2f, \rho = 0$, then

$$G_{21}(x,t) = \frac{1}{6}\sqrt{-1+f^2}(3\sqrt{2}a(-1+e^{f\xi})\rho + i\sqrt{3}\sqrt{f^2+2q-a^2(\eta_1^2+2\rho\mu_1)}).$$

Case 13: If $\mu_1 = 0$, then

$$G_{22}(x,t) = \frac{1}{6}\sqrt{-1+f^2}(\frac{6\sqrt{2}\,a\,\eta\,e^{\rho\,\eta_1}\rho}{2+e^{\xi\eta_1}\rho} + i\sqrt{3}\sqrt{f^2+2q-a^2(\eta_1^2+2\rho\mu_1)}).$$

Case 14: If $2\eta_1 = \mu_1 + \rho$, then

$$G_{23}(x,t) = \frac{1}{6}\sqrt{-1+f^2}(3\sqrt{2}a\mu_1 + \frac{3\sqrt{2}a(-\rho+\mu_1)}{-1+e^{\frac{1}{2}\xi(-\rho+\mu_1)}\rho} + i\sqrt{3}\sqrt{f^2+2q-a^2(\eta_1^2+2\rho\mu_1)}),$$

or

$$G_{24}(x,t) = \frac{1}{12}e^{-2\xi\eta_1}\sqrt{-1+f^2}(3\sqrt{2}a(-1-e^{2\xi\eta_1} + \sqrt{1+6e^{2\rho\eta_1}+e^{4\rho\eta_1}})\rho + 2i\sqrt{3}e^{2\xi\eta_1}\sqrt{f^2+2q-a^2(\eta_1^2+2\rho\mu_1)}).$$

Case 15: If $-2\eta_1 = \mu_1 + \rho$, then

$$G_{25}(x,t) = \frac{1}{6}\sqrt{-1+f^2}(\frac{3\sqrt{2}\,a\,\rho(e^{\frac{1}{2}\xi(-\rho+\mu_1)}+\mu_1)}{e^{\frac{1}{2}(bt+ax)(-\rho+\mu_1)}+\rho} + i\sqrt{3}\sqrt{f^2+2q-a^2(\eta_1^2+2\rho\mu_1)}).$$

Case 16: If $\eta_1 = \rho = 0$, then

$$G_{26}(x,t) = \frac{1}{12}\sqrt{-1+f^2}(3\sqrt{2}\,a\,\xi\,\rho\,\mu_1 + 2i\sqrt{3}\sqrt{f^2+2q-a^2(\eta_1^2+2\rho\mu_1)}).$$

Case 17: If $\eta_1 = \mu_1 = 0$, then

$$G_{27}(x,t) = \frac{1}{6}\sqrt{-1+f^2}(-\frac{6\sqrt{2}a}{\xi} + i\sqrt{3}\sqrt{f^2+2q-a^2(\eta_1^2+2\rho\mu_1)}).$$

Case 18: If $\eta_1 = 0$ and $\mu_1 = \rho$, then

$$G_{28}(x,t) = \frac{1}{12}\sqrt{-1+f^2}(3\sqrt{2}\,a\,\tan(\rho)(C+\xi\mu_1) + 2i\sqrt{3}\sqrt{f^2+2q-a^2(\eta_1^2+2\rho\mu_1)}).$$

Case 19: If $\rho = 0$, then

$$G_{29}(x,t) = \frac{1}{6}\sqrt{-1+f^2}(3\sqrt{2}a\rho(e^{\xi\eta_1} - \frac{\mu_1}{2\eta_1}) + i\sqrt{3}\sqrt{f^2+2q-a^2(\eta_1^2+2\rho\mu_1)}).$$

6. Graphical behavior of wave patterns

This part highlights the model's graphical relevance by presenting 2D, 3D, and contour diagrams together with the results that were produced.

In Figure 1, the 3D, 2D, and contour graphs are shown representing the singular periodic soliton obtained by using trignometric solution $G_1(x,t)$ given in Eq (5.2) with parametric values $\eta_1 = 4$, $\rho = 3$, $f = 3$, $b = 1$, $a = 1$, $\mu_1 = 6$, and $q = 1$. A singular periodic soliton describes a periodic wave with sudden peaks or infinite values at some points. It generally depicts increased non-linearity and potential physical consequences such as localized energy densities or plasma instabilities. Physically, these phenomena can represent repeated high-amplitude waveforms or events of wave collapse, demonstrating the localization of energy at specific points in a non-linear medium. Sharp dark soliton wave behavior of 3D, 2D, and contour graphs is represented by $G_3(x,t)$ in Figure 2, which

is obtained by using the hyperbolic solution discussed in Eq (5.3) with parametric values $\eta_1 = 2, \rho = 1$, $f = 2$, $b = 1$, $a = 1$, $\mu_1 = 1$, and $q = 1$. A sharp dark soliton is an indication of a rapid, localized reduction in wave intensity. A Steep phase shift, high contrast dip, and strong non-linearity are all shown. It is generally stationary and preserves its shape over time due to non-linear and dispersion being in equilibrium. The hyperbolic solution $G_5(x, t)$ of Eq (5.4) gives a kink soliton with parametric values $\eta_1 = 3$, $\rho = -2$, $f = 3$, $b = 1$, $a = 1$, $\mu_1 = 2$, and $q = 1$. The 3D, 2D, and contour graphs of this kink soliton is shown in Figure 3. A kink soliton in a non-linear system is a stable, localized wave representing a smooth transition from a higher state to a lower state. It preserves its shape when it travels or is stationary and connects two different stable equilibrium states. In other physical systems, e.g., ferromagnetic materials, non-linear transmission lines, membranes in biology, and plasma waves, kink solitons are used to model domain walls, phase boundaries, or transition layers. In plasma physics, e.g., they model ion-acoustic shocks, where a slowly modulated plasma density or potential travels stably in time. Sharp dark soliton wave behavior of 3D, 2D, and contour graphs is represented by $G_7(x, t)$ in Figure 4 which is obtained by using the trignometric solution discussed in Eq (5.5) with parametric values $\eta_1 = 4$, $\rho = -2$, $f = 4$, $b = 1$, $a = 1$, $\mu_1 = 2$, and $q = 1$. These solitons, which are solutions to NLPDEs like the ISLW equation, describe wave propagation in particular non-linear mediums. Their particle-like nature and stability qualify them for energy transport and signal modulation in non-linear media. In optical fibers, Bose-Einstein condensates, and fluid mechanics, a dark soliton is commonly observed. It is a stable localized disturbance wherein energy is transferred and not lost. Figure 5 represents the an anti-kink soliton behavior of 3D, 2D, and contour graphs obtained by using the parametric values $\eta_1 = 4$, $\rho = 3$, $f = 2$, $b = 1$, $a = 1$, $\mu_1 = 3$, and $q = 1$ in hyperbolic solution $G_{13}(x, t)$ discussed in Eq (5.6). An anti-kink soliton is a localized and stable wave that propagates from a higher to a lower state. Since non-linearity and dispersion are equal, it is a step down in the system's state and retains its form. They indicate symmetry in the system and imply reversible processes are conceivable. In Figure 6, the 3D, 2D and contour graphs are shown representing singular-shaped soliton obtained by using hyperbolic solution $G_{19}(x, t)$ discussed in Eq (5.7) with parametric values $\eta_1 = 3$, $\rho = 3$, $f = 2$, $b = 1$, $a = 1$, $\mu_1 = 3$, and $q = 1$. Singular-shaped soliton is a highly localized, often spiky or pointed wave in which non-linearity overwhelms to the extent that smoothness is lost. In physical systems, these parameters can indicate bounds of model validity or failure-related instability points. They can, for instance, specify areas where wave-particle interactions become strongly non-linear, thereby giving rise to shock formation, plasma heating, or wave turbulence. The investigation of these solutions is essential to the understanding of critical behaviors and the onset of chaotic dynamics in complex systems.

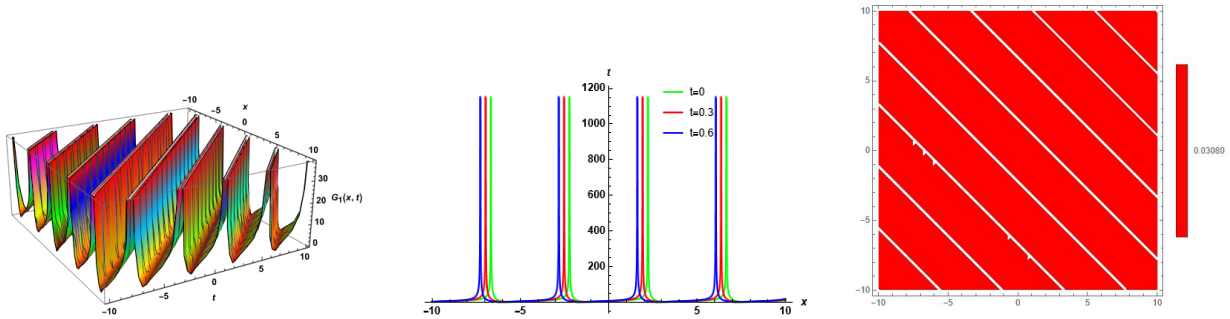

(a) 3D Plot (b) 2D Plot (c) Contour Plot

Figure 1. (a) The 3D animation of the singular periodic wave obtained by using the soliton solution $G_1(x,t)$ discussed in Eq (5.2) is presented, (b) represents a set of 2D line plots illustrating the wave behavior for different values of t, and the contour graph in (c) shows the interdependencies of variables using the parameters $\eta_1 = 4$, $\rho = 3$, $f = 3$, $b = 1$, $a = 1$, $\mu_1 = 6$, and $q = 1$.

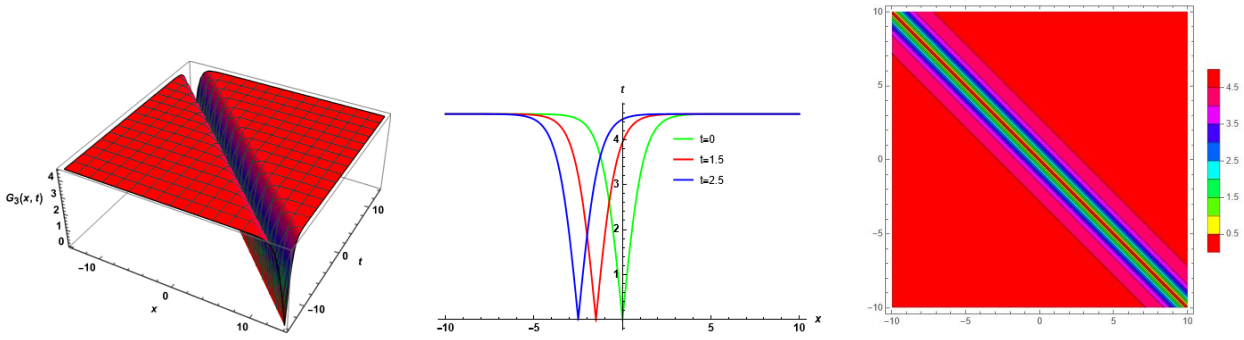

(a) 3D Plot (b) 2D Plot (c) Contour Plot

Figure 2. (a) The 3D animation of the sharp dark soliton wave obtained by using the soliton solution $G_3(x,t)$ given in Eq (5.3) is presented, (b) represents a set of 2D line plots illustrating the wave behavior for different values of t, and the contour graph in (c) shows the interdependencies of variables using the parameters $\eta_1 = 2$, $\rho = 1$, $f = 2$, $b = 1$, $a = 1$, $\mu_1 = 6$, and $q = 1$.

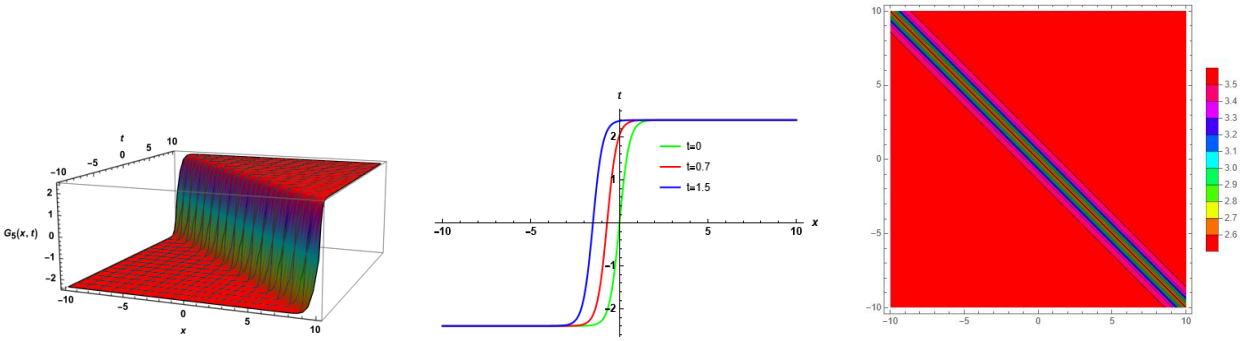

(a) 3D Plot (b) 2D Plot (c) Contour Plot

Figure 3. (a) The 3D animation of the kink soliton wave obtained by using the soliton solution $G_5(x,t)$ discussed in Eq (5.4) is presented, (b) represents a set of 2D line plots illustrating the wave behavior for different values of t, and the contour graph in (c) shows the interdependencies of variables using the parameters $\eta_1 = 3$, $\rho = -2$, $f = 3$, $b = 1$, $a = 1$, $\mu_1 = 2$, and $q = 1$.

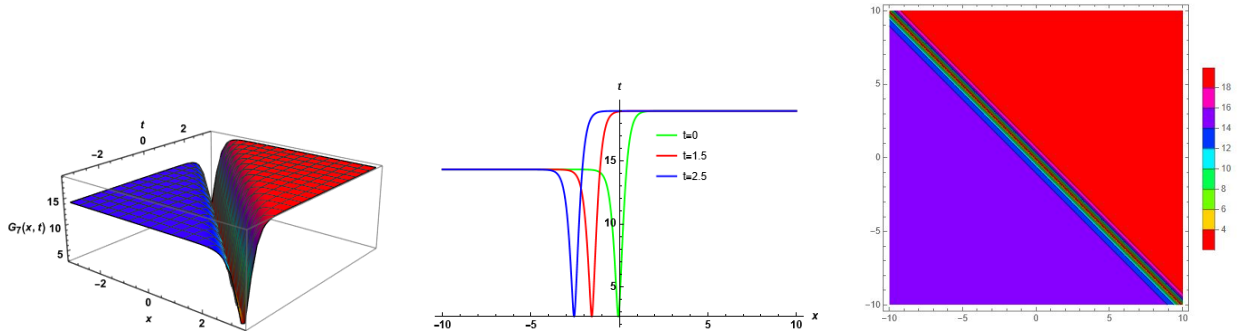

(a) 3D Plot (b) 2D Plot (c) Contour Plot

Figure 4. (a) The 3D animation of the sharp dark soliton wave obtained by using the soliton solution $G_7(x,t)$ discussed in Eq (5.5) is presented, (b) represents a set of 2D line plots illustrating the wave behavior for different values of t, and the contour graph in (c) shows the interdependencies of variables using the parameters $\eta_1 = 4$, $\rho = -2$, $f = 4$, $b = 1$, $a = 1$, $\mu_1 = 2$, and $q = 1$.

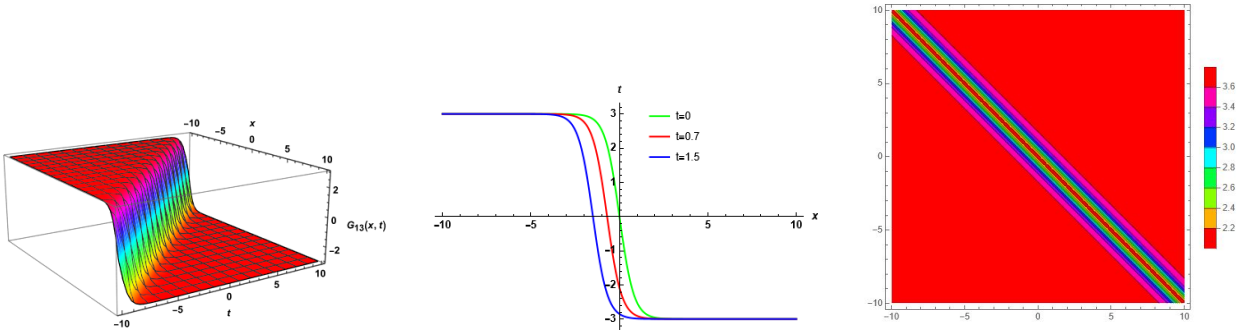

(a) 3D Plot (b) 2D Plot (c) Contour Plot

Figure 5. (a) The 3D animation of the anti kink-type soliton wave obtained by using the soliton solution $G_{13}(x,t)$ discussed in Eq (5.6) is presented, (b) represents a set of 2D line plots illustrating the wave behavior for different values of t, and the contour graph in (c) shows the interdependencies of variables using the parameters $\eta_1 = 4$, $\rho = 3$, $f = 2$, $b = 1$, $a = 1$, $\mu_1 = 3$, and $q = 1$.

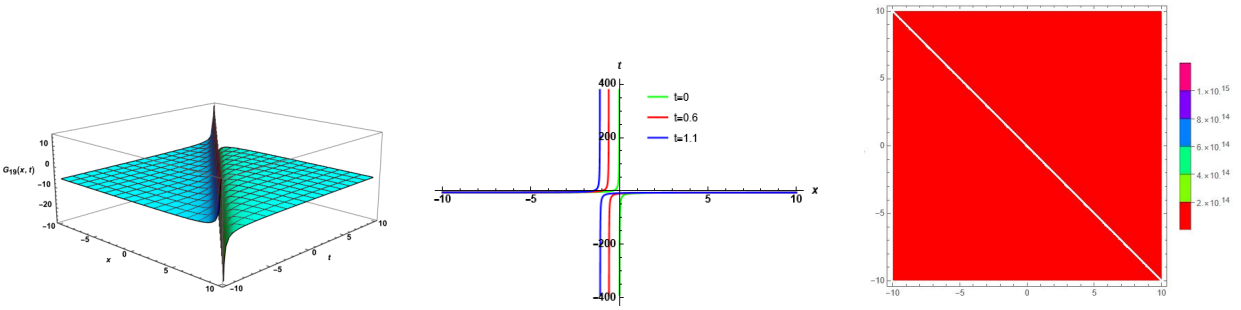

(a) 3D Plot (b) 2D Plot (c) Contour Plot

Figure 6. (a) The 3D animation of the singular shape soliton wave obtained by using the soliton solution $G_{19}(x,t)$ discussed in Eq (5.7) is presented, (b) represents a set of 2D line plots illustrating the wave behavior for different values of t and the contour graph in (c) shows the interdependencies of variables using the parameters $\eta_1 = 3$, $\rho = 3$, $f = 2$, $b = 1$, $a = 1$, $\mu_1 = 3$, and $q = 1$.

7. Bifurcation analysis

This section presents the bifurcation analysis and phase pictures of the planar dynamical system derived for the suggested model. The use of this technique offers a qualitative study of non-linear models. The system's trajectories can be represented by points, simple closed curves, or different isomorphic figures. The equilibrium points are used to examine the emergent dynamics of Eq (3.6). The dynamical system is constructed by letting $G' = R$ and $G'' = R'$.

$$\frac{dG}{d\xi} = R, \frac{dR}{d\xi} = \lambda G + lG^3, \tag{7.1}$$

where $\lambda = \frac{2q+f^2}{a^2}$ and $l = \frac{4}{a^2(f^2-1)}$. This system has the following integral and demonstrates Hamiltonian properties:

$$H(G,R) = \tfrac{1}{2}R^2 - \tfrac{\lambda}{2}G^2 - \tfrac{l}{4}G^4 = h,$$

where h is the Hamiltonian constant.

The equilibrium points of Eq (7.1) are found by solving the resulting set $R = 0$. There is only one equilibrium point $(0, 0)$ found when $\lambda l > 0$. Nevertheless, three equilibrium points are found when $\lambda l < 0$, specifically $(0, 0)$, $(\sqrt{\frac{-\lambda}{l}}, 0)$, $(-\sqrt{\frac{-\lambda}{l}}, 0)$. The Jacobian matrix of Eq (7.1) is:

$$J(G,R) = \begin{vmatrix} 0 & 0 \\ \lambda + 3lG^2 & 0 \end{vmatrix} = -\lambda - 3lG^2.$$

Thus,
(1) (G, R) signifies a saddle point if $J(G, R) < 0$,
(2) (G, R) signifies a central equilibrium if $J(G, R) > 0$,
(3) (G, R) signifies a cuspidal point if $J(G, R) = 0$.
The outcomes that can be achieved by altering the settings are described in the following.

Case 1:

For $\lambda > 0$ and $l > 0$, one equilibrium point $B_1(0, 0)$ can be identified by putting $f = 2, q = 1, a = 1$. The point B_1 donates a saddle point.

Case 2:

For $\lambda < 0$ and $l > 0$, three equilibrium points $B_1(0, 0), B_2(-8, 0), B_3(4, 0)$ can be identified by putting $f = 2, q = -6, a = 2$. The points B_1 and B_3 donate a central equilibrium, whereas the B_2 signifies saddle point.

Case 3:

For $\lambda > 0$ and $l < 0$, three equilibrium points $B_1(0, 0), B_2(4, 0), B_3(-8, 0)$ can be identified by putting $f = 0, q = 1, a = 1$. Both of the points B_1 and B_3 signify saddle points, whereas the point B_2 donates a central equilibrium.

Case 4:

For $\lambda < 0$ and $l < 0$, one equilibrium point $B_1(0, 0)$ can be identified by putting $f = 2, q = -3, a = 1$. The point B_1 donates a central equilibrium.

The visual representation of these cases is given in Figures 7–10.

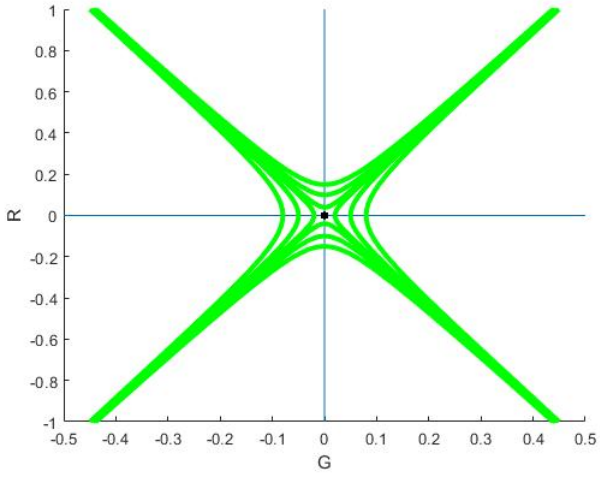

(a)

Figure 7. Phase variation plot. (a): For $\lambda > 0$ and $l > 0$.

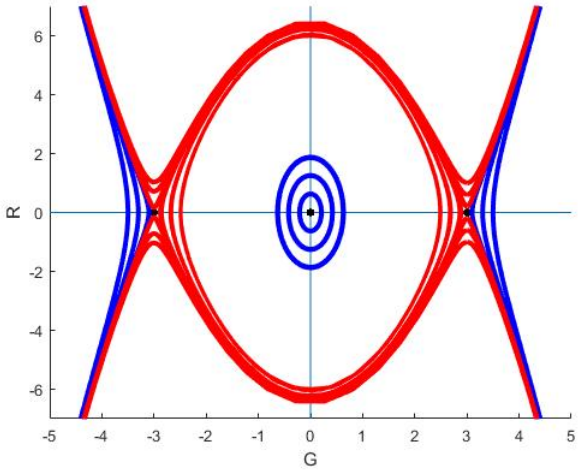

(a)

Figure 8. Phase variation plot. (a): For $\lambda < 0$ and $l > 0$.

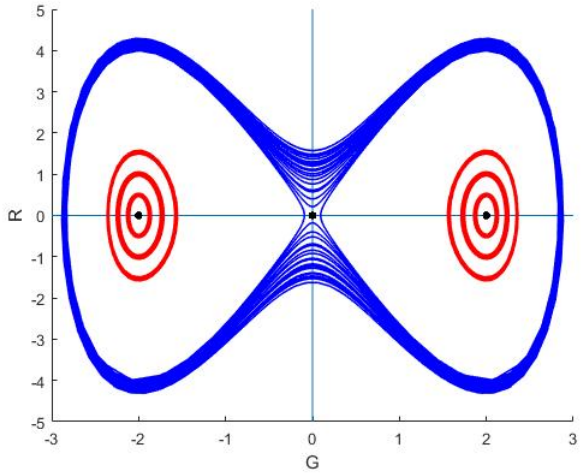

(a)

Figure 9. Phase variation plot. (a): For $\lambda > 0$ and $l < 0$.

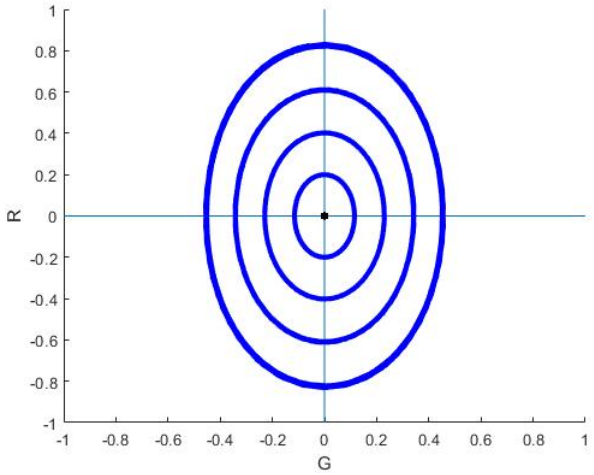

(a)

Figure 10. Phase variation plots. (a): For $\lambda < 0$ and $l < 0$.

8. Chaotic behaviors

This section examines the chaotic behaviors displayed by the model under investigation. The term "chaotic" describes certain dynamics of the system's apparently random behavior that is governed by deterministic laws. Even the smallest changes to the starting conditions might produce very different outcomes. In the end, the trajectories of neighboring points create the system's phase space. Such systems can show underlying shapes or structures, even if their behavior is frequently complex and unpredictable. The concept of chaos theory has significantly changed how we view deterministic

systems and how randomness and predictability occur in nature. Numerous artificial and natural systems, such as fluid dynamics, weather patterns, and optics, can exhibit chaotic behavior. Various disciplines, including physics, biology, engineering, economics, and the social sciences, have used chaos theory. Adding a perturbation term causes Eq (7.1) to behave chaotically. Assuming $\frac{dG}{d\xi} = R$ to start this analysis, the dynamic system is:

$$\frac{dG}{d\xi} = R, \frac{dR}{d\xi} = \lambda G + lG^3 + \beta Cos(\theta t). \tag{8.1}$$

Here, the variable β denotes the magnitude or strength and the symbol θ denotes the frequency or occurrence of the disturbed term. The periodicity, quasi-periodicity, and chaos of the system given in (8.1) have been analyzed through several techniques, such as time and phase plots in 2D and 3D form are illustrated in Figures 11–13.

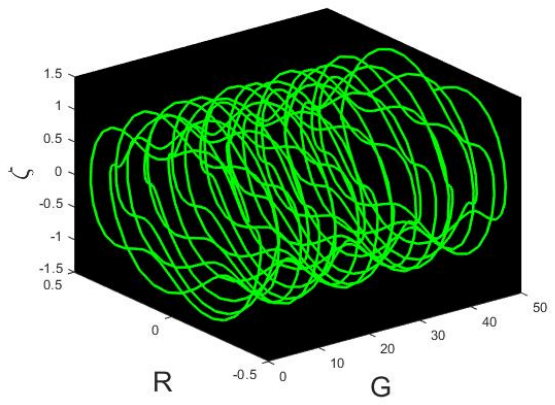

(a) 3D phase plot

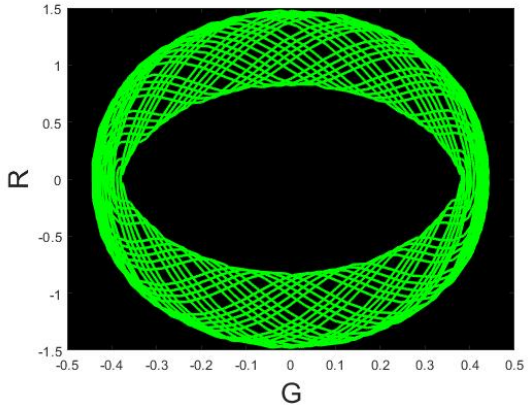

(b) 2D phase plot

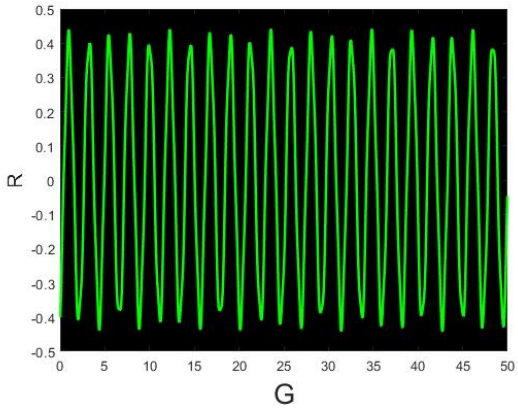

(c) Time series plot

Figure 11. Chaotic behavior of dynamical system (8.1) with parameters $\beta = 3$ and $\theta = 10$.

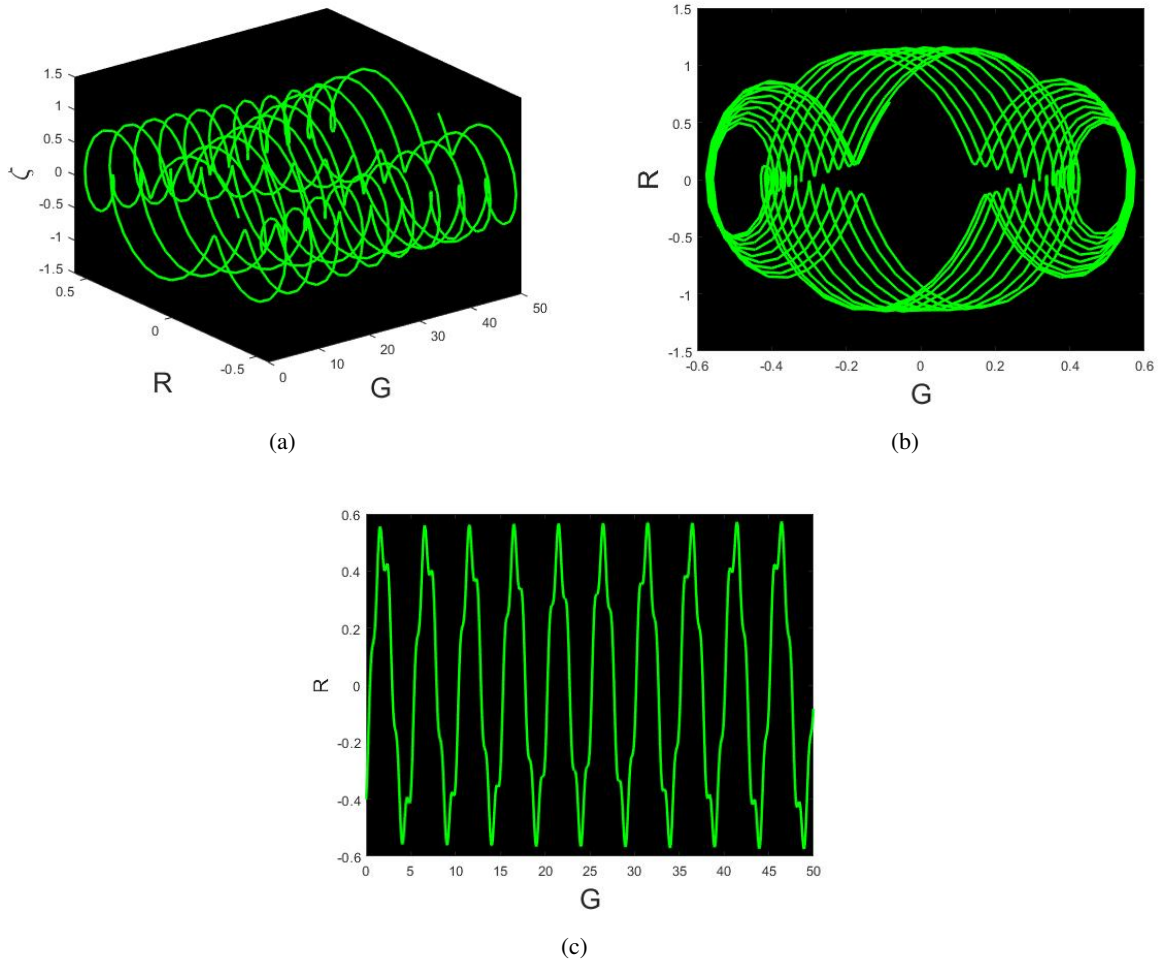

Figure 12. Chaotic behavior of dynamical system (8.1) with parameters $\beta = 3$ and $\theta = 2\pi$.

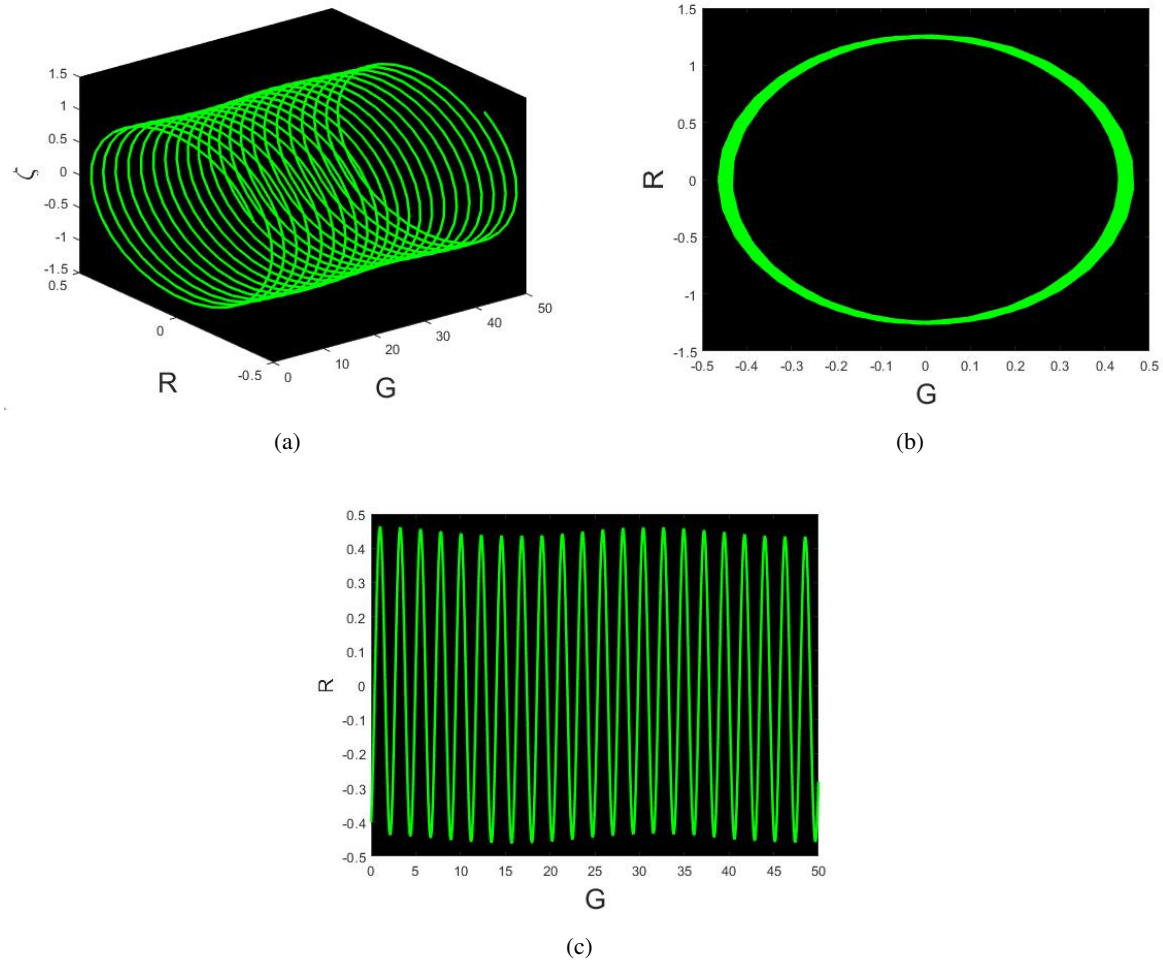

Figure 13. Chaotic behavior of dynamical system (8.1) with parameters $\beta = 0.1$ and $\theta = 0.2$.

9. Sensitivity analysis

Sensitivity analysis is applied in a wide range of applications, including science, engineering, economics, and mathematics, to analyze how variations in model parameters affect the model output. It measures the possible impact of different input sources of uncertainty on the mathematical model output. Sensitivity analysis is helpful to identify which inputs have the most influence on output and how inputs are transmitted through the system. The sensitivity illustrates the non-linearity of the system and indicates how crucial it is to specify the initial conditions precisely to forecast the system's behavior. Sensitivity analysis also helps in understanding the power, reliability, and validity of model predictions that can be used for complex system decision-making. The graphical representation of the sensitivity analysis of the system employed in Eq (8.1), is shown in Figures 14–17.

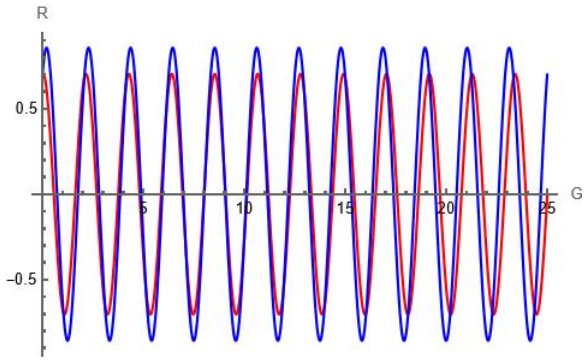

(a)

Figure 14. Sensitivity analysis of dynamical system (8.1) with $(G, R) = (0.7, 0.2)$ for the red curve and $(G, R) = (0.7, 1.5)$ for the blue curve.

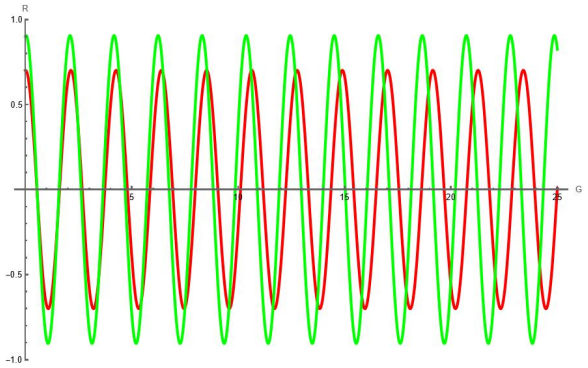

(a)

Figure 15. Sensitivity analysis of dynamical system (8.1) with $(G, R) = (0.7, 0.1)$ for the red curve and $(G, R) = (0.9, 0.3)$ for the green curve.

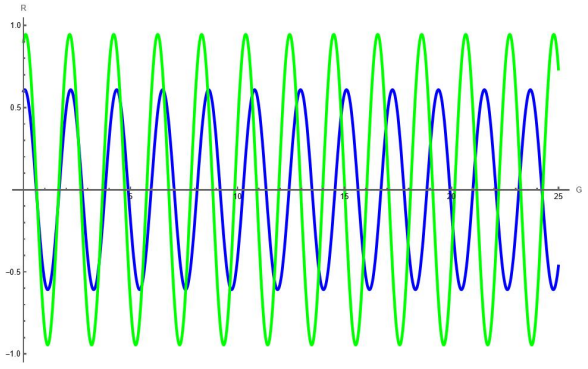

(a)

Figure 16. Sensitivity analysis of dynamical system (8.1) with $(G, R) = (0.6, 0.3)$ for the blue curve and $(G, R) = (0.9, 0.9)$ for the green curve.

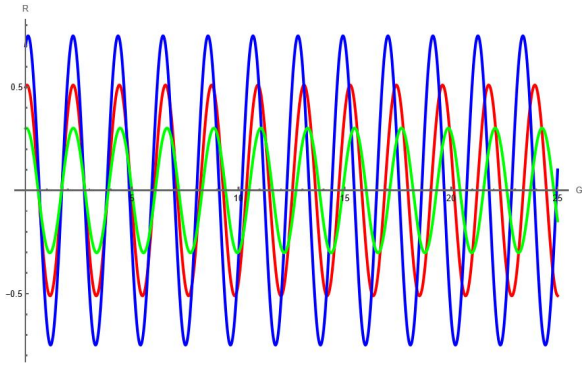

(a)

Figure 17. Sensitivity analysis of dynamical system (8.1) with $(G, R) = (0.5, 0.3)$ for the red curve, $(G, R) = (0.7, 0.8)$ for blue curve and $(G, R) = (0.3, 0.1)$ for the green curve.

10. Conclusions

This research investigated soliton solutions to the ion sound and Langmuir wave model with the the modified Khater method. The method was able to produce valid wave solutions, including singular periodic shape, sharp dark, kink, and anti-kink solitons, significant in the investigation of non-linear wave dynamics in plasmas. The optical soliton solutions obtained through the suggested technique for the ISLW model are different and novel as compared to previous literature. There was a detailed bifurcation analysis to investigate the behavior of the system as the parameters varied. The analysis revealed various dynamic patterns, from periodic oscillations to chaotic behaviors, depending on some conditions. Uncertain behaviors were also investigated through the demonstration that initial conditions or changes in the parameters by a small amount can cause the system to switch between ordered and chaotic dynamics. These findings add to our understanding of non-linear plasma waves, with potential applications in fusion technology, astrophysical plasmas, and wave-based communication. Future research can build upon this work by investigating more complicated multi-wave interactions or the introduction of external influences to create a comprehensive understanding of non-linear wave dynamics.

Author contributions

Marium Khadim: Writing–original draft, Methodology. **Muhammad Abbas:** Supervision, Methodology, Writing–original draft. **Tahir Nazir:** Visualization, Methodology, Writing–original draft. **Alina Alb Lupas:** Visualization, Software, Writing–original draft, Writing–original draft. **Muhammad Nadeem Anwar:** Formal analysis, Visualization, Writing—review and editing. **M. R. Alharthi:** Visualization, Software, Writing—review and editing. All authors have read and approved the final version of the manuscript for publication.

Use of Generative-AI tools declaration

The authors declare they have not used Artificial Intelligence (AI) tools in the creation of this article.

Acknowledgments

The publication of this research was supported by the University of Oradea, Romania. The authors would like to acknowledge the Deanship of Graduate Studies and Scientific Research, Taif University for funding this work.

Conflict of interest

There is no conflict of interest.

References

1. K. Hosseini, F. Alizadeh, E. Hinçal, B. Kaymakamzade, K. Dehingia, M. S. Osman, A generalized nonlinear Schrödinger equation with logarithmic nonlinearity and its Gaussian solitary wave, *Opt. Quant. Electron.*, **56** (2024), 929. https://doi.org/10.1007/s11082-024-06831-8
2. S. T. R. Rizvi, A. R. Seadawy, S. K. Naqvi, M. Ismail, Bifurcation analysis for mixed derivative nonlinear Schrödinger's equation, α-helix nonlinear Schrödinger's equation and Zoomeron model, *Opt. Quant. Electron.*, **56** (2024), 452. https://doi.org/10.1007/s11082-023-06100-0
3. Y. F. Alharbi, A. M. Abd El-Bar, M. A. Abdelrahman, A. M. Gemeay, A new statistical distribution via the Phi-4 equation with its wide-ranging applications, *PloS one*, **19** (2024), e0312458. https://doi.org/10.1371/journal.pone.0312458
4. J. Wang, Z. Li, A dynamical analysis and new traveling wave solution of the fractional coupled Konopelchenko–Dubrovsky model, *Fractal Fract.*, **8** (2004), 341. https://doi.org/10.3390/fractalfract8060341
5. M. M. A. Khater, S. H. Alfalqi, J. F. Alzaidi, R. A. M. Attia, Analytically and numerically, dispersive, weakly nonlinear wave packets are presented in a quasi-monochromatic medium, *Results Phys.*, **46** (2003), 106312. https://doi.org/10.1016/j.rinp.2023.106312
6. M. G. Grillakis, On nonlinear schrödinger equations: nonlinear Schrödinger equations, *Commun. Partial Differ. Equ.*, **25** (2000), 1827–1844. https://doi.org/10.1080/03605300008821569
7. Y. Gu, C. Jiang, Y. Lai, Analytical solutions of the fractional Hirota–Satsuma coupled KdV equation along with analysis of bifurcation, sensitivity and chaotic behaviors, *Fractal Fract.*, **8** (2024), 585. https://doi.org/10.3390/fractalfract8100585
8. Y. Gu, X. Zhang, L. Peng, Z. Huang, Y. Lai, Lump and new interaction solutions of the (3+1)-dimensional generalized Shallow Water-like equation along with chaotic analysis, *Alex. Eng. J.*, **126** (2025), 160–169. https://doi.org/10.1016/j.aej.2025.03.119
9. A. Jhangeer, H. Almusawa, Z. Hussain, Bifurcation study and pattern formation analysis of a nonlinear dynamical system for chaotic behavior in traveling wave solution, *Results Phys.*, **37** (2022), 105492. https://doi.org/10.1016/j.rinp.2022.105492
10. M. Li, L. Wang, F. H. Qi, Nonlinear dynamics of a generalized higher-order nonlinear Schrödinger equation with a periodic external perturbation, *Nonlinear Dyn.*, **86** (2016), 535–541. https://doi.org/10.1007/s11071-016-2906-y

11. L. Tang, A. Biswas, Y. Yildirim, A. Asiri, Bifurcation analysis and chaotic behavior of the concatenation model with power-law nonlinearity, *Contemp. Math.*, **4** (2023), 1014–1025. https://doi.org/10.37256/cm.4420233606
12. N. C. T. Mezamo, V. B. Nana, F. W. Tchuimmo, L. Nana, Stabilization of traveling waves on dissipative system near subcritical bifurcation through a combination of global and local feedback, *Eur. Phys. J. Plus*, **137** (2022), 1139. https://doi.org/10.1140/epjp/s13360-022-03352-9
13. A. R. Seadawy, D. Kumar, K. Hosseini, F. Samadani, The system of equations for the ion sound and Langmuir waves and its new exact solutions, *Results Phys.*, **9** (2018), 1631–1634. https://doi.org/10.1016/j.rinp.2018.04.064
14. H. M. Baskonus, H. Bulut, New wave behaviors of the system of equations for the ion sound and Langmuir Waves, *Waves Random Complex Media*, **26** (2016), 613–625. https://doi.org/10.1080/17455030.2016.1181811
15. A. H. Ganie, A. M. Wazwaz, A. R. Seadawy, M. S. Ullah, H. O. Roshiud, H. D. Afroz, et al., Application of three analytical approaches to the model of ion sound and Langmuir waves, *Pramana–J. Phys.*, **98** (2024), 46. https://doi.org/10.1007/s12043-023-02720-z
16. S. Arshed, G. Akram, M. Sadaf, A. Khan, Solutions of (3+1)-dimensional extended quantum nonlinear Zakharov–Kuznetsov equation using the generalized Kudryashov method and the the modified Khater method, *Opt. Quant. Electron.*, **55** (2023), 922. https://doi.org/10.1007/s11082-023-05137-5

AIMS Press

© 2025 the Author(s), licensee AIMS Press. This is an open access article distributed under the terms of the Creative Commons Attribution License (https://creativecommons.org/licenses/by/4.0)